Lab on a Chip

Dynamic Article Links

Cite this: *Lab Chip*, 2011, **11**, 3619

www.rsc.org/loc

PAPER

MEMS microwell and microcolumn arrays: novel methods for high-throughput cell-based assays†

Po-Cheng Chen,[ab] Yi-You Huang*[a] and Jyh-Lyh Juang*[bc]

Received 15th December 2010, Accepted 12th August 2011
DOI: 10.1039/c0lc00696c

Although the cell-based assay is becoming more popular for high throughput drug screening and the functional characterization of disease-associated genes, most researchers in these areas do not use it because it is a complex and expensive process. We wanted to create a simple method of performing an on-chip cell-based assay. To do this, we used micro-electro-mechanical systems (MEMS) to fabricate a microwell array chip comprised of a glass substrate covered with a photoresist film patterned to form multiple microwells and tested it in two reverse transfection experiments, an exogenous gene expression study and an endogenous gene knockdown study. It was used effectively in both. Then, using the same MEMS technology, we fabricated a complementary microcolumn array to be used as a drug carrier device to topically apply drugs to cells cultured in the microwell array. We tested the effectiveness of microwell–microcolumn on-chip cell-based assay by using it in experiments to identify epidermal growth factor receptor (EGFR) activity inhibitors, for which it was found to provide effective high throughput and high content functional screening. In conclusion, this new method of cell-based screening proved to be a simple and efficient method of characterizing gene function and discovering drug leads.

Introduction

The cell-based assay is now applied to a wide range of biological research topics related to cellular responses to various physiological and pathological stimuli. It allows us to monitor the biochemical activity of target biomolecules in a cellular context without the need for purification and has advantages over conventional enzyme- or antibody-based assays in experiments that require analysis of cell behaviors, including proliferation, differentiation, motility and invasiveness, chemoresistance and changes in cell shape, adhesion, and protein subcellular localization.[1–3] This enables us to simultaneously monitor more than one cellular feature and makes possible the quantification of physiological response data in a real-life cell model. Thus, this information-rich assay can facilitate the efficient and cost-effective discovery of drug leads or drug targets.

Many cell-based assays are now used as part of high throughput screening (HTS) in biological pathway studies and drug lead screenings,[4,5] for which from tens to hundreds of thousands of samples require analysis. For this, multiwell microplates in 96- and 384-well formats are often used. These microplates increase the density of the wells per plate as well as reduce the volume of reaction agents needed. However, the increased density of wells per plate presents technical challenges in the handling of liquid and the detection of targets. To resolve this problem, cell-based screening is often automated to reduce the time and cost of manual interventions.[6] Most of these automation systems are expensive to develop, making them only affordable for large research groups or large pharmaceutical companies. Therefore, there is an emerging need for a simple, robust, and reliable cell-based assay for HTS for the world's researchers, most of whom are not working in such well-funded laboratories.

Transfection microarray represents a significant advance in the miniaturization and simplification of high-throughput assays of gene functions.[7] To genetically probe the function of genes, cultured cells are dropped uniformly over an entire array chip, where cells are reversely transfected with expression plasmids or siRNAs pre-spotted on the slide, for ectopic expression or knockdown of endogenous gene, respectively.[7–9] In this well-less cell array, however, the locally transfected cells are actually surrounded by non-transfected cells, making it difficult to separate the transfected cells from the non-transfected cells. In addition, this 2D cell microarray does not confine the cell growth and cell movement within the transfected region and thus the spacing between two neighboring transfected cell clusters in the slide should be large enough to maintain the border of cell

[a]*Institute of Biomedical Engineering, College of Engineering, College of Medicine, National Taiwan University, No.1, Sec.1, Jen-Ai Road, Taipei, 100, Taiwan. E-mail: yyhuang@ntu.edu.tw*
[b]*Division of Molecular and Genomic Medicine, National Health Research Institutes, 35, Keyan Road, Zhunan Town, Miaoli County, 350, Taiwan*
[c]*PhD Program for Aging, China Medical University, Taichung, 40402, Taiwan. E-mail: juang@nhri.org.tw*

† Electronic supplementary information (ESI) available. See DOI: 10.1039/c0lc00696c

clusters in long-term cell culture. Another challenge facing this cell microarray technology is how to use it for drug screening. The well-less cell microarray does not allow topical application of small molecular drugs onto a restricted zone in the slide without cross-contamination.

To overcome these problems, cell growth needs to be confined, which could be achieved with the use of miniaturized wells. Such a concept has been attempted by several groups recently. For example, a high-density (9216 wells) microwell array is fabricated by titanium coating on the glass slide for siRNA reverse transfection assays,[10] a PMMA-bottom microwell array fabricated by a micromilling process for the analysis of cell microsphere production,[11] a sandwiched microwell–micropost assay for drug screening,[12] and 24- and 96-well versions of single cell gel electrophoresis array for DNA damage analysis.[13]

Here, we report our use of a MEMS-based process to fabricate a high-density (65 800 wells) microwell structure that could adhere to the glass slide to perform cell-based gene expression and siRNA assays. We also fabricated a microcolumn array to carry and release small molecular drugs into the microwells, mimicking the conventional topical application of drugs into the microplate by pipetting. Using this MEMS array, we performed a proof-of-concept study that would require on-chip cell-based drug screening. We found this novel cell-based assay system to be powerful, versatile, and easily used for HTS of gene function and drug leads.

Materials and methods

Microarray chip fabrication

The microwells and microcolumns were fabricated using negative photoresist materials, SU-8 100, SU-8 2050 and SU-8 3050 (MicroChem), according to manufacturer's directions. Briefly, photomasks were used to block photoresist exposure to UV radiation in selected areas which had been spun onto pre-cleaned glass wafers (Tekstarter). The photoresist materials were then developed and air-dried with nitrogen to form an array structure consisting of either multiple concave microwells or convex microcolumns (Fig. 1A). Using a dicing saw, we cut the wafers into chips with the size of a standard microscope slide (75 mm × 25 mm).

Adhesion test

We surface-sterilized the fabricated microarray chips with UV-C irradiation for 15 min before placing them into 100 mm culture dishes filled with Minimum Essential Media culture medium (GIBCO). To ensure every microwell was fully filled with culture medium, the culture dish was degassed at 25 mbar vacuum for five min. After the microarray chips had been immersed in the culture medium at 37 °C for 48 to 72 h, they were removed from the culture dish and examined by a dissecting microscope to ensure the MEMS-fabricated structure had attached to the glass slide.

Plasmid and cell lines

The pCMV–GFP–DsRed plasmid, which encodes a fusion protein of GFP–DsRed, was constructed by PCR amplification of DsRed from pDsRed-Express-1 (Clontech) and cloned into the pGFP2 vector. The stable HeLa cell line overexpressing EGFP–DsRed was produced by transfecting pCMV–EGFP–DsRed into HeLa 229. We selected only transformants that were resistant to Zeocin. The H1299 lung cancer cell line overexpressing EGFR L858R mutant protein was a gift from Dr Yi-Rong Chen (NHRI, Taiwan). H1299 and HeLa 229 cells were grown in MEM supplemented with 10% FCS, and the 293T cells were grown in Dulbecco's Modified Eagle's Medium (GIBCO) supplemented with 10% FCS.

Reverse transfection with cDNA or siRNA

Reverse transfection on the microwell array was performed using liposome-based transfection reagents as described previously.[7,9] Briefly, 1 μg EGFP plasmid was mixed with 4 μl of Lipofectamine 2000 (Invitrogen) in 15 μl OptiMEM (Invitrogen) supplemented with 0.2 M sucrose. After incubation at room temperature (RT) for 10 min, the DNA–liposome complex was then mixed homogeneously with 5 μl of 0.125% gelatin (Sigma). By using a contact microarray printer (DNA Array06G2, Wittech Co.), the gelatin–DNA mixture was spotted onto a 2666-well microarray chip. The microwell chip was transferred into a culture dish, and 12 ml of 293T cells at a density of 1.65×10^5 cells per ml was added to cover the microwell array by drop cell seeding. A light vacuum was applied to ensure homogeneous cell seeding. The microwell chip was transferred to a tissue culture incubator (37 °C, 5% CO_2) for 48 h and the EGFP expression was then analyzed by a fluorescent microscope (Leica, TCS SP5).

For reverse transfection experiments, 5 to 50 ng of GFP-siRNA or non-target siRNA (Purigo) and 3 μl of RNAiMAX (Invitrogen) were mixed with 11 μl OptiMEM supplemented with 0.2 M sucrose and incubated for 15 min at RT. 12 ml of HeLa 229 cells at a density of 8.3×10^4 cells per ml was added to cover the microwell chip. The rest of the experiment followed the same procedures as described above for the reverse transfection of EGFP. At 72 h post-transfection, the fluorescent signals were detected by fluorescent microscopy.

Drug treatment by the microcolumn

The microcolumn array was pre-treated with 0.01% poly-L-lysine (PLL) (Sigma) before coating. The microcolumns were coated with concentrations (0.2 to 20 mM) of pyrrolidine dithiocarbamate (PDTC) (Sigma) mixed with 20 μl of 1% alginate or 0.3% gelatin and dried for 16 h at 4 °C. The microwell array chip was sterilized by UV irradiation before being placed into a 100 mm culture dish. 12 ml of HeLa 229 cells at 2.5×10^5 cells per ml density was added into the culture dish to cover the microwell array chip, which was then incubated at 37 °C, 5% CO_2 overnight.

The microcolumn array was then inserted into the microwell array to release drugs into the microwells. The alignment of microcolumn to microwell was carried out by using an align pedestal (1.35 mm in diameter) and a complementary align cavity (1.5 mm in diameter) fabricated at the four corners of the microcolumn and microwell arrays, respectively (Fig. S1†). After matching the align positions, the four pedestals on the microcolumn array were slowly slipped into the four corresponding

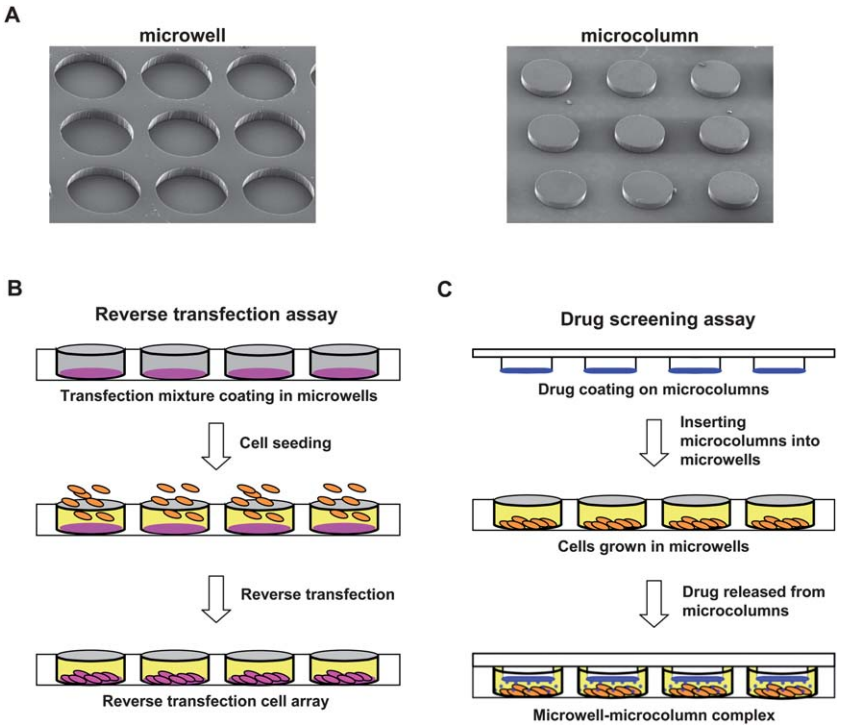

Fig. 1 SEM images and schematic illustration of the methodology for cell-based functional assays. (A) SEM micrographs of the MEMS fabricated microwell (left panel) and microcolumn arrays (right panel). The MEMS microarray device comprises a MEMS film that forms a coating material on a transparent glass substrate in such a way that it creates a plurality of microwells or microcolumns arranged in spatially discrete regions on the glass surface. (B) and (C) show the procedures for the on-chip functional assay. (B) The workflow for reverse transfection in the microwell array. Transfection mixture containing a protein expression plasmid or synthetic siRNA, transfection reagents, and gelatin was spotted onto the bottom of microwells. Cell seeding was performed by drop seeding of suspension cells directly onto microwell arrays. At 72 h post-transfection, the fluorescent signal of the target gene was examined by a microscope. (C) The workflow for drug treatment with microcolumns. Small molecular drugs mixed in 1% alginate or 0.3% gelatin were coated onto PLL-treated microcolumns. After drying at 4 °C for 16 h, the microcolumn array was inserted into the microwell array and the microcolumn–microwell complex was then placed in a humidified chamber and incubated at 37 °C, 5% CO_2 until cell immunolabeling and fluorescent imaging.

cavities on the microwell array. The microcolumn–microwell array complex was placed in a humidified chamber and incubated at 37 °C, 5% CO_2 for 4 h. The microwell array was then detached from the complex and rinsed three times with PBS buffer, following incubation with 20 ng ml^{-1} TNF-α (PeproTech) for 30 minutes at 37 °C, 5% CO_2. Immunoassay was performed to detect subcellular localization of NF-κB with anti-NF-κB p65 antibody (Santa Cruz).

We then wanted to try a small scale drug screening test. To do this, we added 12 ml of H1299 cells expressing L858R mutant proteins at 3×10^5 cells per ml density to the sterilized microwell array and incubated it at 37 °C under 5% CO_2 overnight. Three positive controls known to inhibit EGFR activity, AG1478 (Calbiochem), PP2 (Calbiochem), and gefitinib (LC Laboratories), and 76 existing pharmacologically active compounds from the Library of Pharmacologically Active Compounds collection (Sigma) were mixed with 2% alginate or 0.5% gelatin to a final concentration of 1 mM each before dispensing onto the microcolumns by a microarray printer (DNA Array06G2, Wittech Co.). The microcolumn–microwell array complex was incubated at 37 °C, 5% CO_2 for 1 h. Anti-myc (American Type Culture Collection) and anti-phospho-EGFR (Tyr1068) (Cell Signaling) antibodies were used for the immunoassay.

Image acquisition and statistical analysis

The fluorescent images of cells in response to drug treatment were automatically taken by an ImageXpress Micro System (Molecular Devices, CA, USA) with 40× objective lens. The digital fluorescent images were then analyzed using MetaXpress Software (Molecular Devices) set for multi-wavelength cell scoring. For statistical analysis, experiments were repeated two to three times with duplicate samples for each experimental condition. The Student's *t*-test was used to evaluate significance of two independent samples ($p < 0.05$). All error bars represent the standard error of the mean.

Results and discussion

Fabrication of MEMS-based microwell and microcolumn arrays

In this study, we used MEMS based technology to fabricate a microwell structure with miniaturized wells for cell cultures and to fabricate a microcolumn structure to be used to release drugs into the wells of the microwell array. Scanning electron microscopy (SEM) was used to observe the 3D morphology of the microwell and microcolumn structures (Fig. 1A). As diagramed in Fig. 1B and C, we used the microwell array for a gene function study and the microwell array plus microcolumn array for a drug

screening study. To use the microwell array for reverse transfection, the transfection mixture containing either cDNA or synthetic siRNA and the transfection reagent was coated onto the bottom of microwells before cell seeding. Two to three days post-transfection, cells were fixed and fluorescence microscopy was performed with conventional microplates (Fig. 1B). We used the microcolumn array in a drug release study (Fig. 1C). Briefly, microcolumns were pre-coated with small molecular drugs and inserted into the microwells where cells had been grown in culture medium (Fig. 1C). Using this microcolumn for drug release makes it possible to add numerous drugs to all the microwells at the same time without introducing time lag, an important advantage over conventional robotic manipulator arm which adds drugs one row at a time by pipetting.

Adhesion test of microwell arrays in cell culture medium

A transparent-substrate bottom is required for the image analysis of cell-based assays. However, unlike silicon wafer, the glass wafer provides a poor bonding surface for the photoresist film.[14] A standard vapor primer like hexamethyldisilane could possibly be used to enhance adhesion of the photoresist film to the wafer surface but it is biotoxic and hydrophobic and may cause cell death or prevent cells from attaching onto the microwells. Thus, it is critical to select a photoresist material that would adhere to the glass wafer without this vapor primer. Among various thick photoresists used for MEMS, the SU-8 series negative photoresists are probably best suited to cell-based analysis due to their biocompatibility.[15] However, we noted that some SU-8 photoresists such as SU-8 2050 films can easily peel away from the glass wafer of the fabricated microwell structure after storage in air at RT for few days (data not shown). We tested the adhesion of SU-8 100 and SU-8 3050 to the glass wafers in fabricated microwell array chips in culture medium to determine the stability of photoresist–substrate interface during cell-based assay. The attachment of SU-8 3050 to the glass wafer was found to be intact after 72 h immersion in culture medium, while that of SU-8 100 was found to have detached at 48 h (Fig. S2†). These data suggest that the SU-8 3050 fabricated microwell structure stably binds to the glass wafer without any hydrophobic polymer coating. Thus, such a device is biocompatible and stable for cell culturing.

Cell culturing in the microwell array

To test whether this microwell structure could provide a proper environment for cell culturing, we fabricated 2666-well (Fig. 2A) and 65 800-well (Fig. 2B) arrays for cell culture assay. Cell seeding was performed by drop seeding 293T cells directly onto microwell arrays. After 48 h incubation, cell number and morphology were imaged by fluorescent microscopy. The 2666-well array had 350–500 cells per well (Fig. 2C), and the 65 800-well array had 30–50 cells per well (Fig. 2D). Importantly, this platform does not require an automated high throughput cell plating system for uniform cell seeding in microwells.

To examine the consistency of cell densities across the microwell array, we plated out HeLa 229 cells into a 2666-well chip. After 48 h culture, cells were labeled with Hoechst 33342 to determine the cell number. We found that cell densities in

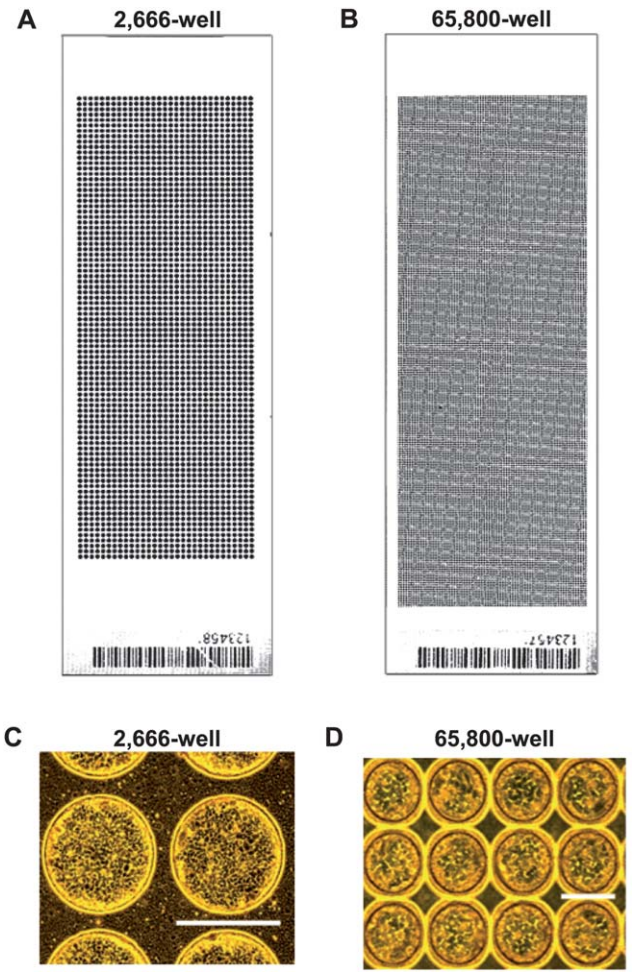

Fig. 2 Cell culturing test using microwell arrays. (A) and (B) are microscope images of the 2666-well and 65 800-well arrays before the cell culturing test, respectively. For the 2666-well array, the diameter and spacing between adjacent wells are 500 μm and 100 μm, respectively, and for 65 800-well array are 120 μm and 20 μm, respectively. (C) The phase-contrast images of 293T cells grown on a 2666-well array chip. The cell number per well was about 350–500 cells. (D) The cell number of 293T cells grown on a 65 800-well array chip was about 30–50 cells per well. Scale bars, 500 μm (C) and 120 μm (D).

microwells across the chip appeared to be relatively consistent (Fig. S3A†). For statistical analysis, we selected 62 wells each from exterior and interior regions to examine their cell densities by an ImageXpress Micro System (Molecular Devices, CA, USA) with 10× objective lens. The results showed that the cell densities in exterior and interior wells were 260 ± 39 and 265 ± 29 cells per well, respectively (p-value 0.36) (Fig. S3B†), suggesting that there is no significant difference between these two groups. Thus, this microwell array platform does not require an automatic dispenser system for homogeneous cell seeding into microwells.

To determine whether the cell morphology in microwells is comparable to that in conventional 96-well microplates, we examined living cells by phase-contrast microscopy to observe cell proliferation throughout the culture period. For a better morphological analysis, cells cultured for 24 h were immunolabeled by rhodamine phalloidin to determine whether there is

a morphological difference between cells grown in a macroscopic plate and a microwell array. The phase-contrast and fluorescence images showed no visible difference when HeLa 229 cells were cultured in a microwell chip compared to that in a flat-bottom 96-well plate (Fig. S4†). Furthermore, we also investigated if a regional difference in cell morphology is present in this array. We sampled microwells from exterior and interior regions for cell imaging and found micrograph images of phase-contrast, Hoechst nuclear staining, and rhodamine phalloidin actin immunolabelling were all comparable between different array regions (Fig. 3). These findings suggest that the MEMS microwell arrays can be used to perform cell-based assays. Since one 65 800-well array assay is equivalent to 685 assays conducted with the conventional 96-well plate, it dramatically increases cell-based assay throughput and efficiency. Although it is possible to fabricate an even higher density of microwell on the array chip, the cell number would fall below 30 cells per well (with a diameter of 120 μm) for large size cells. Because the individual variation of cell phenotype could be large in cell-based assays, a sample size below 30 cells per well could limit the power of statistical analysis. Thus, the capacity of 65 800-well array probably approaches the upper limit for cell-based assays.

Reverse transfection in the microwell array

The functions of a large number of genes identified in human genome project have yet to be investigated. Understanding their functions provides new avenues for advances in understanding disease processes and the development of new therapeutic procedures. Thus, it is of interest to test whether the microwell array fabricated in this study can be used for reverse transfection. Using this microwell array, we performed reverse transfection assay with a plasmid expressing EGFP in 293T cells. We found microwell to microwell transfection efficiency (about 40%) at 72 h post-transfection to be comparable, based on GFP fluorescent signal (Fig. 4A, left panel). We also performed the same assay with siRNA. A stable cell line overexpressing EGFP–DsRed fusion protein was reversely transfected with chemically synthesized EGFP siRNA in microwells to find out if repression of EGFP expression would consequently diminish the DsRed signal of the EGFP–DsRed fusion protein. At 72 h postinfection, we found a clear dose-dependent decrease of the DsRed signal by GFP-siRNA (Fig. 4B, upper panel). Together, these results suggest that the MEMS microwell array chip can be used in cell-based assay studies of gene function.

Drug release by the microcolumn array

Functional cell-based assay has recently become a preferred choice of screening in drug discovery.[5,6] To test whether the microwells can actually segregate fluids during the drug treatment by microcolumns, we coated sequential rows of microcolumns with alternating soluble fluorescent dyes of Cy3 and Cy5. The microwell array was filled with cell culture medium and the drips coming out of the array were dried with a sterilized lens

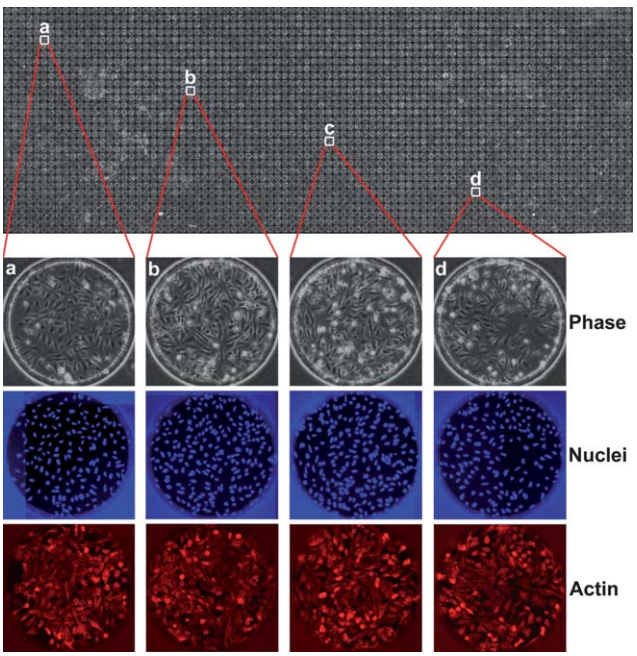

Fig. 3 Cell seeding test. HeLa 229 cells were seeded in a 2666-well array chip. After 48 h incubation, cells were immunolabeled with Hoechst and Rhodamine phalloidin, and cell morphologies were observed by phase-contrast and fluorescent microscopies. We sampled four microwells from different regions (a, b, c, and d) for cell imaging and found micrograph images of phase-contrast, Hoechst nuclear staining, and rhodamine phalloidin actin immunolabelling were all comparable between different chip regions.

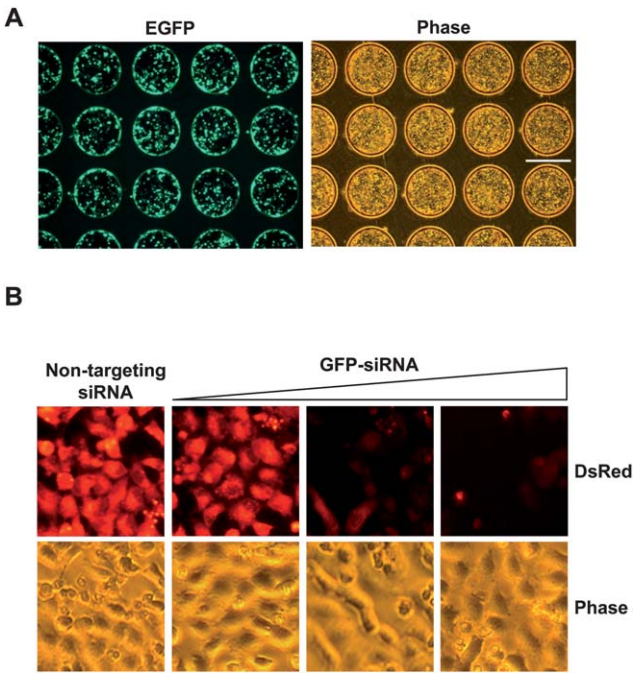

Fig. 4 Reverse transfection experiments using a 2666-microwell array. (A) Reverse transfection of an EGFP expression plasmid in 293T cells. At 72 h post-transfection, the microscope images showed the transfection efficiency to be comparable between microwells, as judged by the EGFP fluorescent signal. Scale bar, 500 μm. (B) Reverse transfection assay with siRNA. The HeLa cells stably expressing EGFP–DsRed fusion protein were reversely transfected with GFP-siRNA at final concentrations of 0.25, 1 and 2.5 ng μl^{-1} in the microwells. At 72 h postinfection, the fluorescent micrographs revealed an obvious decrease of the DsRed signal by GFP-siRNA in a dose-dependent manner (upper panel).

paper from the bottom edge of the array. To avoid overflow of liquids between wells, the level of medium was reduced to half in microwells, by placing the microwell array into a 10 cm culture dish for air drying in a laminar flow hood for 10–15 min. We then inserted the microcolumns into the microwells for 1 h, and photographed the fluorescent images of microwells using an Axon Scanner. The results indicated that the Cy3 and Cy5 signals did not overlap each other, suggesting that the microwells indeed segregated fluids individually (Fig. S5†).

To test whether our MEMS microcolumn array could function as a drug release device in performance of cell-based assays, we coated a NF-κB activity inhibitor, PDTC,[16] onto the microcolumn, lined up the microcolumn array over the microwell array, and then immersed the microcolumns into the microwells growing HeLa cells. We chose to test NF-κB activity because it can be triggered by a variety of signals, including TNF-α.[16,17] This activates NF-κB which translocalizes into the nucleus for the transcriptional regulation of target genes involved in inflammatory responses. Four hours after the PDTC treatment with the microcolumn array, cells in microwells were treated with TNF-α for 30 min to induce NF-κB translocation. Cells were double immunolabelled with anti-NF-κB and a nucleus dye (Hoechst 33342) to determine NF-κB subcellular localization. Confocal microscropy images showed that NF-κB was translocalized into nucleus by TNF-α and PDTC treatment inhibited the NF-κB translocation in a dose-dependent manner (Fig. 5A, upper panel). To quantify the NF-κB translocation, we analyzed the fluorescent signals using a high-throughput image analysis software. The numerical values of the quantified image signal also agreed with the visual impression of the fluorescent images (Fig. 5B). These data suggest that the microcolumn array can be used in on-chip cell-based assays for drug screening. In addition, this array platform also eliminates the need for using an automation system to dispense and/or to aspirate multiple reagents from microwells for immunofluorescent staining.

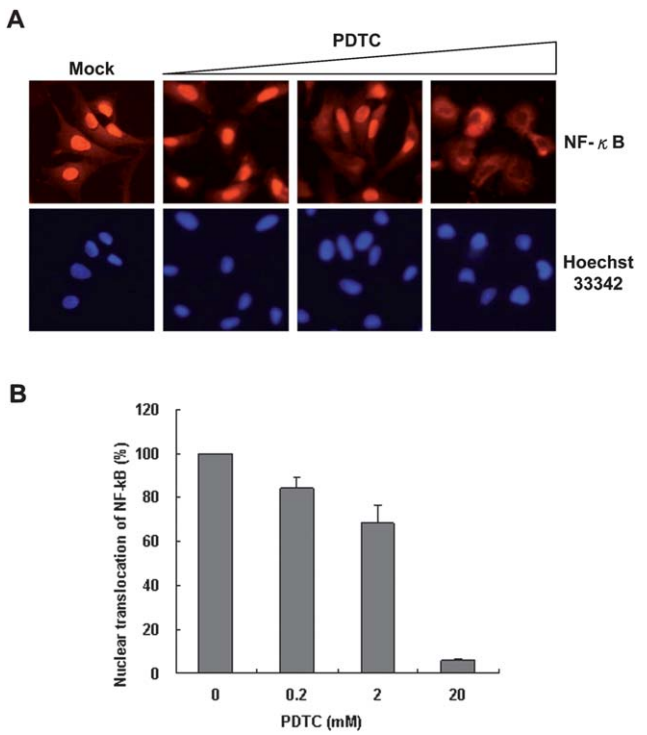

Fig. 5 Drug treatment with the microcolumn array. (A) HeLa 229 cells grown in microwells at 2.5×10^5 cells per ml density were treated with 0.2 to 20 mM PDTC coated on the microcolumn array for 4 h and then incubated with 20 ng ml^{-1} TNF-α for 30 minutes before immunolabeling the subcellular localization of NF-κB with anti-NF-κB p65 antibody. A dose-dependent inhibition of TNF-α-induced NF-κB nuclear translocation by PDTC was noted. (B) Quantification of the NF-κB nuclear location using MetaXpress software.

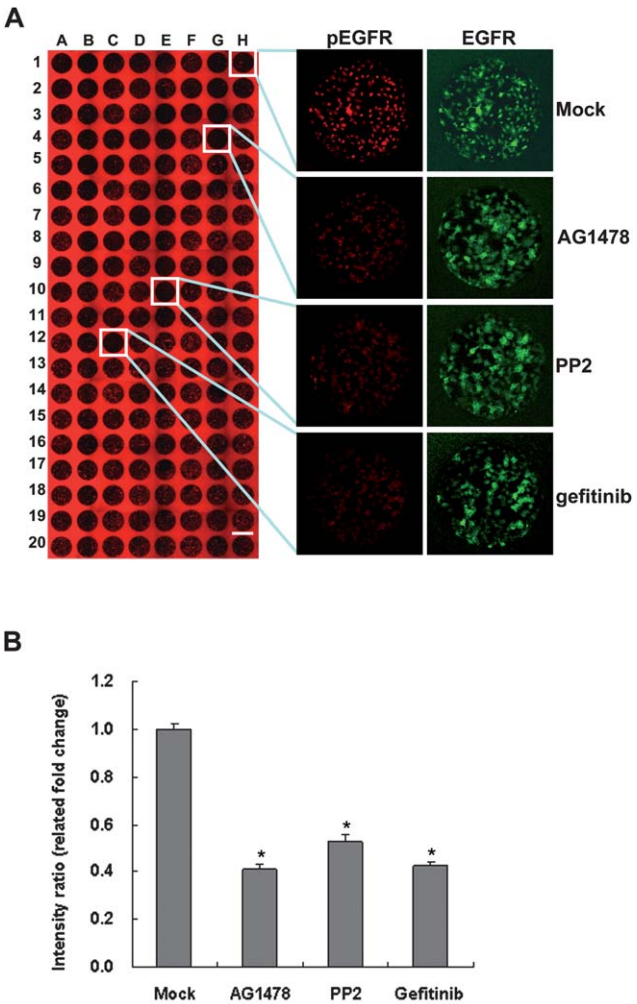

Fig. 6 A proof-of-concept drug screening for EGFR activity inhibitors. (A) The EGFR-L858R overexpressing lung cancer H1299 cells grown in a block of 20 × 8 microwells were treated for 1 h with a total 79 pharmacologically active compounds coated on the microcolumn. The EGFR activity was represented by the phospho-EGFR signal by double immunostaining with anti-phospho-EGFR and anti-EGFR antibodies. Higher magnification images of phospho-EGFR (red) and EGFR (green) for the cells in the microwells are boxed in the left panel. The three positive controls, including gefitinib, AG1478, and PP2, displayed substantial activity in repressing the phospho-EGFR signal compared to mock control (right panel). (B) Quantification of the fluorescent image. The fluorescent signals were scanned by an ImageXpress Micro System and data were analyzed using MetaXpress Software to quantify the results. The three positive controls showed significant activity ($p < 0.05$) in the inhibition of EGFR activity.

An on-chip cell-based screening of EGFR activity inhibitors

It was of interest to perform a proof-of-concept study to demonstrate the feasibility of these MEMS arrays for drug screening. We choose to perform a small scale screening test for the EGFR inhibitors because over-expression of EGFR promotes tumor growth in lung cancer and the EGFR-target therapies have recently been introduced to treat lung cancers. However, given that EGFR-target therapies often develop drug resistance,[18] the development of an alternative approach to indirectly target EGFR activity has been proposed.[19] Interestingly, constitutive EGFR phosphorylation level can be an indicator of higher EGFR kinase activity and also a surrogate marker predicting a patient's clinical response to a clinical EGFR inhibitor (gefitinib). Taking advantage of this feature, we conducted a small scale drug screening for the EGFR inhibitors with the EGFR-L858R mutant lung cancer cell line, which has been reported previously to be more responsive to gefitinib.[20] We coated the microcolumn with a total of 79 different small molecular drugs, including three known EGFR inhibitors (gefitinib, AG1478, and PP2)[19,21] plus 76 pharmacologically active compounds. These small molecular drugs were coated in duplicate in a block of 20 × 8 microcolumns. The cells in microwell array were treated with the drugs coated on the microcolumn for one hour before double immunostaining with anti-phospho-EGFR and anti-EGFR antibodies to determine the cellular EGFR activity. As expected, the three positive controls exhibited comparable activity in suppressing the phospho-EGFR signal compared to the mock control (Fig. 6A, right panel). We also scanned and analyzed the fluorescent signals to quantify the results and found only that the three positive controls displayed significant activities ($p < 0.05$) in inhibiting the EGFR activity (Fig. 6B). The rest of 76 small molecular compounds did not appear to notably suppress the phospho-EGFR signal (Table S1†). Our data demonstrate the validity of this novel cell-based assay system for functional analysis of specific targeted proteins in drug lead screening.

Although we found the microwell array and microcolumn array that we fabricated are able to perform cell-based studies that had previously been performed by prohibitively expensive automatic machines, more work needs to be done to improve the liquid dispenser's ability to position and dispense such low volumes of reagents into the MEMS fabricated microwell and microcolumn microstructures.

Conclusion

The cell-based assay has several advantages. First, it requires only a single incubation step for functional screening, making the workflow simple and efficient. Second, it can be used with various current commercial automated imaging and informatics systems. Third, because this cell-based assay system can greatly reduce the reagent volume to 1/3000 of that used by 96-well plate assay, it can drive down cost per sample. Finally, because a single array chip assay may potentially allow up to 65 800 samples to be analyzed simultaneously, throughput is dramatically increased. With the increasing demand for functional screens from the global drug discovery industry, this MEMS array system has the potential of accelerating the process of drug discovery.

Acknowledgements

We thank Dr De-Yao Wang, Dr Yueh-Ying Hsu, Shiou-Ling Jian, Shu-Hui Wu and Huan-Yi Tseng for their technical assistance. We also thank Dr Yi-Rong Chen for providing reagents for this work and James Steed for English editing assistance.

References

1 B. Angres, *Expert Rev. Mol. Diagn.*, 2005, **5**, 769–779.
2 M. K. Hancock, L. Kopp and K. Bi, *Assay Drug Dev. Technol.*, 2009, **7**, 68–79.
3 N. Misawa, A. K. Kafi, M. Hattori, K. Miura, K. Masuda and T. Ozawa, *Anal. Chem.*, 2010, **82**, 2552–2560.
4 P. A. Clemons, *Curr. Opin. Chem. Biol.*, 2004, **8**, 334–338.
5 J. C. Engel, K. K. Ang, S. Chen, M. R. Arkin, J. H. McKerrow and P. S. Doyle, *Antimicrob. Agents Chemother.*, 2010, **54**, 3326–3334.
6 P. J. Zhu, W. Zheng, D. S. Auld, A. Jadhav, R. Macarthur, K. R. Olson, K. Peng, H. Dotimas, C. P. Austin and J. Inglese, *Comb. Chem. High Throughput Screening*, 2008, **11**, 545–559.
7 J. Ziauddin and D. M. Sabatini, *Nature*, 2001, **411**, 107–110.
8 S. Mousses, N. J. Caplen, R. Cornelison, D. Weaver, M. Basik, S. Hautaniemi, A. G. Elkahloun, R. A. Lotufo, A. Choudary, E. R. Dougherty, E. Suh and O. Kallioniemi, *Genome Res.*, 2003, **13**, 2341–2347.
9 X. Cheng, A. Guerasimova, T. Manke, P. Rosenstiel, S. Haas, H. J. Warnatz, R. Querfurth, W. Nietfeld, D. Vanhecke, H. Lehrach, M. L. Yaspo and M. Janitz, *Gene*, 2010, **450**, 48–54.
10 J. Reymann, N. Beil, J. Beneke, P. P. Kaletta, K. Burkert and H. Erfle, *BioTechniques*, 2009, **47**, 877–878.
11 Y. Sakai, S. Yoshida, Y. Yoshiura, R. Mori, T. Tamura, K. Yahiro, H. Mori, Y. Kanemura, M. Yamasaki and K. Nakazawa, *J. Biosci. Bioeng.*, 2010, **110**, 223–229.
12 J. Wu, I. Wheeldon, Y. Guo, T. Lu, Y. Du, B. Wang, J. He, Y. Hu and A. Khademhosseini, *Biomaterials*, 2011, **32**, 841–848.
13 D. K. Wood, D. M. Weingeist, S. N. Bhatia and B. P. Engelward, *Proc. Natl. Acad. Sci. U. S. A.*, 2010, **107**, 10008–10013.
14 P. V. R. D. C. S. Bien, S. J. N. Mitchell and H. S. Gamble, *J. Micromech. Microeng.*, 2003, **13**, S34–S40.
15 G. Voskerician, M. S. Shive, R. S. Shawgo, H. von Recum, J. M. Anderson, M. J. Cima and R. Langer, *Biomaterials*, 2003, **24**, 1959–1967.
16 H. W. Ziegler-Heitbrock, T. Sternsdorf, J. Liese, B. Belohradsky, C. Weber, A. Wedel, R. Schreck, P. Bauerle and M. Strobel, *J. Immunol.*, 1993, **151**, 6986–6993.
17 H. L. Pahl, *Oncogene*, 1999, **18**, 6853–6866.
18 S. Kobayashi, T. J. Boggon, T. Dayaram, P. A. Janne, O. Kocher, M. Meyerson, B. E. Johnson, M. J. Eck, D. G. Tenen and B. Halmos, *N. Engl. J. Med.*, 2005, **352**, 786–792.
19 Y. N. Fu, C. L. Yeh, H. H. Cheng, C. H. Yang, S. F. Tsai, S. F. Huang and Y. R. Chen, *Oncogene*, 2008, **27**, 957–965.
20 S. Tracy, T. Mukohara, M. Hansen, M. Meyerson, B. E. Johnson and P. A. Janne, *Cancer Res.*, 2004, **64**, 7241–7244.
21 X. F. Zhu, Z. C. Liu, B. F. Xie, Z. M. Li, G. K. Feng, D. Yang and Y. X. Zeng, *Cancer Lett.*, 2001, **169**, 27–32.